HHS Public Access

Author manuscript

Ann Thorac Surg. Author manuscript; available in PMC 2016 November 01.

Published in final edited form as:

Ann Thorac Surg. 2015 November ; 100(5): 1556–1562. doi:10.1016/j.athoracsur.2015.04.109.

Comparison of hemodynamics after aortic root replacement using valve-sparing or bioprosthetic valved conduit

Jeremy D Collins, MD[1], **Edouard Semaan, MD**[1], **Alex Barker, PhD**[1], **Patrick McCarthy, MD**[3], **James C Carr, MD**[1], **Michael Markl, PhD**[1,2], and **S. Chris Malaisrie, MD**[3]

[1]Department of Radiology, Feinberg School of Medicine, Northwestern University, Chicago, USA

[2]Department Biomedical Engineering, McCormick School of Engineering, Northwestern University, Chicago, USA

[3]Division of Cardiac Surgery, Feinberg School of Medicine, Northwestern University, Chicago, IL

Abstract

Background—The purpose is to compare aortic hemodynamics and blood flow patterns using in-vivo 4D flow MRI in patients following valve-sparing aortic root replacement (VSARR) and aortic root replacement with bio-prosthetic valves (BIO-ARR).

Methods—In-vivo 4D flow MRI was performed in 11 patients after VSARR (47±18 years, 6 BAV, 5 TAV), 16 patients after BIO-ARR (52±14 years), and 10 healthy controls (47±16 years). Analysis included 3D blood flow visualization and grading of helix flow in the ascending aorta (AAo) and arch. Peak systolic velocity was quantified in 9 analysis planes in the AAo, aortic arch, and descending aorta. Flow profile uniformity was evaluated in the aortic root and ascending aorta.

Results—Peak systolic velocity (2.0–2.5m/s) in the aortic root and AAo in both VSARR and BIO-ARR were elevated compared to controls (1.1–1.3m/s, $p < 0.005$). Flow asymmetry in BIO-ARR was increased compared to VSARR, evidenced by more AAo outflow jets (9 of 16 BIO-ARR, 0 of 11 in VSARR). BIO-ARR exhibited significantly ($p<0.001$) increased helix flow in the AAo as a measure of increased flow derangement. Finally, peak systolic velocities were elevated at the aortic root for BIO-ARR (2.5 vs 2.0m/s, $p < 0.05$) but lower in the distal AAo when compared to VSARR..

Conclusion—VSARR results in improved hemodynamic outcomes when compared with BIO-ARR as indicated by reduced peak velocities in the aortic root and less helix flow in the AAo by 4D flow MRI. Longitudinal research assessing the clinical impact of these differences in hemodynamic outcomes is warranted.

Address for Correspondence: S, Chris Malaisrie, MD., Department of Cardiac Surgery, Northwestern University, 201E. Huron St, Galter 11-140, Chicago, Illinois 60611, USA, Phone: +1 312-695-2517, Fax: +1 312-926-5991, malaisrie@northwestern.edu.

Introduction

The estimated incidence of thoracic aortic aneurysms (TAA) is 6 per 100,000 person-years, most commonly involving the aortic root and/or the ascending aorta (AAo). Complications associated with TAA include intramural hematoma, aortic dissection, and aortic rupture. To prevent these complications consensus guidelines recommend surgical correction when the aortic diameter exceeds 5.5 cm in patients with trileaflet aortic valves (TAV) and 5.0 - cm in patients with bicuspid aortic valve (BAV) and risk factors for acute aortic syndrome [1–3].

Surgical options for aortic root aneurysm include aortic root replacement with a valved-conduit where both the aortic wall and valve are replaced or valve-sparing aortic root replacement, replacing only the aortic wall. Despite the technical success of both procedures, the impact of the surgical technique on post-repair hemodynamics is poorly understood. It is unclear which procedure provides the most optimal hemodynamic outcome as defined by a normal range of aortic peak velocities and restoration of cohesive aortic outflow. Although previous studies have investigated the mechanics of reimplanted aortic valves [4] only a small number of studies have analyzed in-vivo three-directional blood flow in the thoracic aorta and assessed the potential consequences of the surgically altered aortic geometry and compliance [5–11].

Previous reports based on time-resolved 3D phase contrast MRI (4D flow MRI) suggest that this novel technique can provide information on the temporal evolution of 3D blood with full volumetric coverage of the thoracic aorta over the cardiac cycle [9,12]. Recent studies that have investigated aortic hemodynamics include analysis of vortex flow in the sinuses of Valsalva following different valve-sparing aortic root replacement procedures. This work has contributed to an ongoing discussion about the physiologic role of the sinuses and the importance of maintaining sinus geometry [13]. Additionally, blood flow patterns and turbulence downstream from a prosthetic aortic valve have been found to be dependent on the specific valve design [5– 8,10,13,14].

Understanding the hemodynamic consequences of these surgical procedures has the potential to identify surgical strategies that result in more physiologic post-operative thoracic aortic blood flow. We hypothesize that post-surgical thoracic aortic blood flow is more physiologic in patients following valve-sparing aortic root replacement (VSARR) than bio-prosthetic valves (BIO-ARR), with more uniform flow profiles, less helical flow, a lower incidence of jet flow, and reduced peak systolic velocities throughout the thoracic aorta.

Material and Methods

This retrospective study was approved by our local institutional review board (#STU61320).

Study cohort

Our study cohort was comprised of n=37 subjects divided into three groups. Group 1 included patients after VSARR with re-implantation of their native bicuspid aortic valve (n=6, age=42±18 years, 5 men, pre-surgical aortic diameter = 4.7±1.3cm) and tricuspid aortic valve (n=5, age=55±21 years, 4 men, aortic diameter =5.1±0.2cm). Group 2 (n=16)

consisted of patients who underwent BIO-ARR (age=52±14 years, 15 men, pre-surgical aortic diameter = 4.6±0.48cm). Group 3 (n=10) consisted of healthy volunteers (age 47±16 years, 7 men). The following demographic data and risk factors for TAA were obtained from the electronic medical record: body mass index (BMI), systolic and diastolic blood pressure (BP), resting heart rate, history of dyslipidemia, history of hypertension, and the left ventricular ejection fraction (LVEF).

Surgical Technique

Valve-sparing aortic root replacement—VSARR was performed using a modified reimplantation technique, as described previously. Dacron grafts to replace the aortic root ranged in size from 28 to 36 mm in order to recreate neo-sinuses. The coronary arteries were anastomosed to the Dacron graft as buttons. A second smaller graft was used to replace the tubular segment of the ascending aorta. Hemiarch repair was performed when the proximal aortic arch diameter was >4.0 cm. Valve repair was performed at the discretion of the surgeon and predominantly involved free margin plication. The coronary arteries were anastomosed to the Dacron graft as buttons.

Aortic root replacement—BIO-ARR was performed using a modified Bentall procedure. The composite valve-graft was constructed using a stented bovine pericardial valve sewn on the bottom of Dacron graft. The graft size was typically 5 or 7 mm larger than the valve size. Horizontal mattress sutures with pledgets on the ventricular side were passed through the aortic annulus (non-everting technique) then through both the sewing ring of the valve and the bottom of the Dacron graft. The coronary arteries were anastomosed to the Dacron graft as buttons.

The following perioperative characteristics were recorded for BIO-ARR and VSARR groups: perfusion time (min), cross-clamp time (min), CABG (%), post-operative length of stay (days), pre-discharge complications (%), and 30-day mortality (%). The number of VSARR subjects who underwent aortic valve repair was recorded.

MR Imaging

All studies were performed on 1.5T or 3T MRI systems. Contrast-enhanced prospectively ECG-gated 3D MRA was performed to assess aortic dimensions. Aortic hemodynamics were evaluated using time-resolved 3D phase-contrast (PC) MRI with three directional velocity encoding (4D flow MRI) measuring 3D blood flow velocities with full volumetric coverage of the thoracic aorta. 4D flow MRI was acquired during free breathing using respiratory and prospective ECG gating covering the entire thoracic aorta in an oblique sagittal orientation as described previously [16].

Aortic Valve Morphology and Function

Aortic valve morphology and function was determined by reviewing CINE balanced steady state free precession and 2D PC MR images obtained at the level of the aortic valve. BAV morphology was classified according to Sievers [17]. Aortic valve stenosis and regurgitation were classified as trace, mild, moderate, or severe as described per published guidelines [3].

Thoracic Aortic Size

Pre-surgical aortic dimensions were quantified on a dedicated 3D workstation with multiplanar reformatting capabilities (Vitrea, Vital Images, Minneapolis, MN).

3D Blood Flow Visualization

4D flow MRI data was pre-processed using a workflow described previously [18]. A 3D PC MRA was calculated from 4D flow MRI and combined with 3D blood flow visualization to overlay blood flow onto the vascular anatomy. Aortic blood flow patterns were evaluated using time-resolved 3D pathlines enabling the visualization of time-resolved blood flow throughout the cardiac cycle. Systolic 3D streamlines were calculated to visualize the 3D distribution of the measured three-directional velocities across individual time-frames (Figure 1). Traces were color-coded by the local blood flow velocity using a standard color look up scale.

Helical Flow

4D-blood flow visualization was performed in a blinded fashion by a single observer. Visualization analysis included a semi-quantitative assessment of helix flow and outflow jet patterns. Helix flow was considered rotational motion around the longitudinal axis of the vessel centerline (i.e. the physiologic flow direction) creating a corkscrew-like flow pattern. Helical flow was assessed in the ascending thoracic aorta, aortic arch, and descending thoracic aorta. The grade of helical flow was assessed on a 3-point ordinal scale: 0, small helix formation (flow rotation <180°); 1, moderate supra-physiologic helix (180° < flow rotation <360°); 2, prominent supra-physiologic helix (flow rotation >360°).

Flow Profile Uniformity and Peak Systolic Velocity Quantification

For each patient, 3D PC-MRA data was used to manually position nine analysis planes at defined anatomical landmarks distributed throughout the ascending aorta, aortic arch, and descending thoracic aorta [18]. Analysis planes were placed at the following positions (Figure 2B): Plane 1 at the aortic root distal to the aortic valve, plane 2 in the proximal ascending aorta (AAo), plane 3 in the AAo at the level of the pulmonary artery, plane 4 in the AAo proximal to the origin of the brachiocephalic trunk, plane 5 between the origins of the brachiocephalic trunk and left common carotid artery, plane 6 between the origins of the left common carotid and left subclavian arteries, plane 7 in the proximal descending aorta (DAo), plane 8 in the DAo at the level of plane 1, and plane 9 in the distal DAo. The peak systolic velocity was calculated for all analysis planes. Flow profile uniformity, defined as symmetry of systolic flow profiles was evaluated in analysis planes 1–3. Flow profiles were assessed by dividing the aortic cross sections into quadrants. A single observer identified quadrants with systolic peak velocities >1m/sec in each of these three analysis planes across the cohorts.

Statistical Analysis

Between-group differences for continuous variables were assessed with the student’s t-test. Differences between categorical variables were assessed using the Chi-squared test. A p-

value <0.05 was considered statistically significant; all tests were performed using a two-tailed analysis.

Results

Study Cohort

Patient preoperative demographic data is summarized in Table 1. No subjects had severe aortic stenosis or insufficiency. As assessed with CMR, three (18%) BIO-ARR subjects had moderate aortic insufficiency prior to surgery; all other subjects had mild or less aortic insufficiency. Three BIO-ARR patients (18%) had moderate aortic stenosis; all other BIO-ARR patients did not have aortic stenosis pre-surgery. Five (45%) of VSARR patients demonstrated mild aortic insufficiency. No VSARR subjects demonstrated moderate or severe regurgitation or aortic stenosis at baseline.

BIO-ARR patients demonstrated a larger baseline thoracic aortic size compared to the VSARR patients (average 5.2±0.3 vs. 4.8±1.1cm, p=0.005). Significant differences were also noted regarding the baseline heart rates for VSARR compared to BIO-ARR subjects (p=0.007). Of the six VSARR subjects with BAV (55%), two (33%) and four (67%) demonstrated Sievers type 0 and type 1 morphology, respectively.

BIO-ARR and VSARR surgical characteristics are compared in Table 2. Surgical characteristics were available in 15 (94%) of BIO-ARR and 9 (82%) of VSARR patients. VSARR surgeries required significantly longer perfusion time and cross-clamp time; there were no significant differences in post-surgery length of stay, pre-discharge complications, or 30-day mortality between groups. The majority of VSARR subjects (n=8, 89%) underwent aortic valve repair at the time of aortic root repair.

3D Blood Flow Visualization and Helical Flow

4D flow MRI was successfully employed to visualize 3D blood flow in the thoracic aorta of all n=37 subjects. Representative thoracic aortic blood flow visualization emphasizing qualitative differences between groups is depicted in Figure 1. Semi-quantitative image grading of all 3D visualization data revealed significantly increased helical flow in the ascending aorta of BIO-ARR patients compared to both VSARR patients and control subjects, independent of aortic valve morphology (Table 3).

Flow Profile Uniformity, Systolic Peak Velocity Quantification

3D blood flow visualization demonstrated increased flow asymmetry in BIO-ARR patients (Figure 2A), consistent with a higher prevalence of AAo outflow jets (9 of 16 BIO-ARR patients, 0 of 11 in VSARR patients). Noticeably, the valve sparing approach restored more cohesive outflow as indicated by less eccentric flow profiles and complete absence of ascending aortic flow jets impinging the aortic wall in all VSARR subjects as opposed to the BIO-ARR group. All control subjects demonstrated uniform flow profiles.

Results of systolic peak velocity quantification are summarized in figure 2B. High systolic peak velocities ≥2m/s at the aortic root and proximal AAo were found in both BIO-ARR and VSARR groups compared to control subjects (1.1–1.3m/s, $p < 0.005$). For both patient

groups, peak systolic velocities were significantly elevated throughout the AAo, arch, and proximal DAo (analysis planes 1–7, $p<0.0001$ to $p<0.05$). In addition, BIO-ARR patients demonstrated significantly increased peak systolic velocities at the aortic root (2.5 vs 2.0m/s, $p < 0.05$). Conversely, VSARR patients demonstrated higher velocities in the distal AAo (1.8 vs 1.4m/s, $p < 0.05$) with a trend towards higher velocities in the arch.

Comment

This study demonstrates the potential of 4D flow MRI to assess blood flow patterns in the thoracic aorta as a surrogate outcome measure in patients undergoing aortic valve surgery at the time of aortic root aneurysm repair. Our study compared metrics of aortic hemodynamics (helix flow, flow asymmetry, peak systolic velocities) along the entire thoracic aorta for patients who underwent VSARR and BIO-ARR and compared these results with those of healthy volunteers as a measure of physiologic aortic blood flow. The findings of our study provide evidence that, compared to BIO-ARR, VSARR resulted in more physiological hemodynamics within the ascending aorta yielding reduced forward flow impingement on the AAo wall. Both groups showed increased systolic peak velocities compared to values found in control subjects (on the order of 1.3m/s). Noticeably, BIO-ARR patients had significantly higher peak systolic velocities at the aortic root suggesting differential valve function compared to VSARR.

High peak systolic velocities for both groups throughout the thoracic aorta are likely a consequence of replacing of part of the ascending aorta with graft material (Figure 2B) changing compliance of the vessel. We speculate that the reduced compliance of the aortic graft martial compared to native aortic tissue and thus absence of the normal physiological Windkessel effect resulted in increased velocities. This hypothesis is supported by studies evaluating compliance mismatch between implanted grafts and native vessels in the peripheral arteries as a cause for graft failure through the promotion of intimal hyperplasia at the graft anastomosis [19,20]. A number of studies have shown that left ventricular outflow results in right handed helical flow in the ascending aorta during ventricular systole, as a normal physiological phenomenon [21]. For example, normal aortic helical flow typically involves a flow rotation of <180°. In our cohort, helical flow was identified in the majority of BIO-ARR patients but was rare in patients following VSARR indicating favorable hemodynamics following valve repair with re-implantation. However, pronounced helix flow (grading > 1) as only observed in three BIO-ARR subjects (18%) demonstrates that both surgical techniques can restore relatively cohesive 3D blood flow in the majority of cases with more physiologic post-operative hemodynamics observed following VSARR.

Recent studies have provided evidence that the more common morphology of right-non-coronary cusp and right-left coronary cusp fusion results in eccentric forward flow jets which impinge on the anterior aortic root and the mid ascending aorta respectively with the attendant risk of aneurysm development in these locations [22–25]. With this in mind, following VSARR and BIO-ARR, patients consistently demonstrated higher velocities along the right anterior quadrant of the mid ascending aorta, in the region of the anastomosis, which could increase the risk of aneurysm development in this region. Previous work by our group demonstrated similar blood flow patterns independent of aortic valve morphology

suggesting that resuspension of bileaflet aortic valves yielded similar post-operative blood flow patterns to resuspended trileaflet aortic valves [13].

The non-physiologic aortic blood flow, as seen in both VSARR and BIO-ARR groups in our study is of uncertain clinical significance. Increased peak velocities, flow asymmetry, and helical flow leads to increased viscous energy losses, increasing the load on the heart. The extent of viscous energy loss has been evaluated in the context of TAA and aortic valve stenosis, compared to healthy volunteers. In this study there was significantly increased viscous energy loss in both aortic dilation and aortic stenosis compared to healthy volunteers [26]. Other investigators have quantified turbulent energy loss using 4D flow MRI in aortic stenosis [27] and assessed flow derangements across valve prostheses in vitro [14]. These studies suggest that the combined effects of viscous and turbulent energy loss increase the workload on the heart; however longitudinal studies of the impact of such loading are lacking. Available longitudinal follow-up data in patients who underwent aortic valve replacement suggest an increased risk of aortic dissection and aortic aneurysm in follow-up [28].

Limitations

This study has several important limitations. The retrospective study design precluded capture of all patient surgical characteristics as some patients were referred to our institution for follow-up care after surgical treatment. Direct comparison of baseline to post-surgical quantitative flow imaging was not possible as a minority of patients underwent 4D flow MRI as part of their baseline assessment. Consequently, a comparison cohort of healthy volunteers was used to assess the normalization of aortic hemodynamics following VSARR or BIO-ARR. Our group has previously demonstrated similar hemodynamic outcomes following VSARR in TAV and BAV patients, permitting their grouping into a single cohort for comparison to BIO-ARR [13].

Conclusion

The results of our study suggest that 4D flow MRI can be successfully employed to evaluate the hemodynamic outcome by measuring time-resolved 3D blood flow in the thoracic aorta following VSARR and BIO-ARR. Aortic root replacement increases peak systolic velocities not only in the aortic root and ascending aorta, but also in the arch in both VSARR and BIO-ARR patients. Flow appears to be more physiologic in the VSARR groups with less helix flow and eccentric flow profiles compared to BIO-ARR. The long-term effects of such hemodynamic changes are not fully understood and additional follow-up studies are warranted to investigate the longitudinal outcomes on valve durability and aortic physiology.

Acknowledgments

NIH NHLBI grants R01HL115828 and NIH K25HL119608; Additional support by the Northwestern's Bicuspid Aortic Valve Program at the Bluhm Cardiovascular Institute.

References

1. Hiratzka LF, Bakris GL, Beckman JA, Bersin RM, Carr VF, Casey DE Jr, et al. 2010 ACCF/AHA/AATS/ACR/ASA/SCA/SCAI/SIR/STS/SVM guidelines for the diagnosis and management of

patients with Thoracic Aortic Disease: a report of the American College of Cardiology Foundation/American Heart Association Task Force on Practice Guidelines, American Association for Thoracic Surgery, American College of Radiology, American Stroke Association, Society of Cardiovascular Anesthesiologists, Society for Cardiovascular Angiography and Interventions, Society of Interventional Radiology, Society of Thoracic Surgeons, and Society for Vascular Medicine. Circulation. 2010; 121(13):e266–e369. [PubMed: 20233780]

2. Erbel R, Aboyans V, Boileau C, Bossone E, Bartolomeo RD, Eggebrecht H, et al. 2014 ESC Guidelines on the diagnosis and treatment of aortic diseases. 2014
3. Nishimura RA, Otto CM, Bonow RO, Carabello BA, Erwin JP 3rd, Guyton RA, et al. 2014 AHA/ACC Guideline for the Management of Patients With Valvular Heart Disease: A Report of the American College of Cardiology/American Heart Association Task Force on Practice Guidelines. Circulation. 2014
4. Leyh RG, Schmidtke C, Sievers HH, Yacoub MH. Opening and closing characteristics of the aortic valve after different types of valve-preserving surgery. Circulation. 1999; 100(21):2153–2160. [PubMed: 10571974]
5. David TE, Armstrong S, Ivanov J, Feindel CM, Omran A, Webb G. Results of aortic valve-sparing operations. J Thorac Cardiovasc Surg. 2001; 122(1):39–46. [PubMed: 11436035]
6. David TE, Feindel CM. An aortic valve-sparing operation for patients with aortic incompetence and aneurysm of the ascending aorta. J Thorac Cardiovasc Surg. 1992; 103(4):617–621. discussion 622. [PubMed: 1532219]
7. de Oliveira NC, David TE, Ivanov J, Armstrong S, Eriksson MJ, Rakowski H, et al. Results of surgery for aortic root aneurysm in patients with Marfan syndrome. J Thorac Cardiovasc Surg. 2003; 125(4):789–796. [PubMed: 12698141]
8. Karck M, Kallenbach K, Hagl C, Rhein C, Leyh R, Haverich A. Aortic root surgery in Marfan syndrome: Comparison of aortic valve-sparing reimplantation versus composite grafting. J Thorac Cardiovasc Surg. 2004; 127(2):391–398. [PubMed: 14762346]
9. Markl M, Draney MT, Miller DC, Levin JM, Williamson EE, Pelc NJ, et al. Time-resolved three-dimensional magnetic resonance velocity mapping of aortic flow in healthy volunteers and patients after valve-sparing aortic root replacement. J Thorac Cardiovasc Surg. 2005; 130(2):456–463. [PubMed: 16077413]
10. Yun KL, Miller DC, Fann JI, Mitchell RS, Robbins RC, Moore KA, et al. Composite valve graft versus separate aortic valve and ascending aortic replacement: is there still a role for the separate procedure? Circulation. 1997; 96(9 Suppl):II-368–II-375.
11. Kvitting JP, Ebbers T, Wigstrom L, Engvall J, Olin CL, Bolger AF. Flow patterns in the aortic root and the aorta studied with time-resolved, 3-dimensional, phase-contrast magnetic resonance imaging: implications for aortic valve-sparing surgery. J Thorac Cardiovasc Surg. 2004; 127(6): 1602–1607. [PubMed: 15173713]
12. Markl M, Kilner PJ, Ebbers T. Comprehensive 4D velocity mapping of the heart and great vessels by cardiovascular magnetic resonance. J Cardiovasc Magn Reson. 2011; 13:7. [PubMed: 21235751]
13. Semaan E, Markl M, Chris Malaisrie S, Barker A, Allen B, McCarthy P, et al. Haemodynamic outcome at four-dimensional flow magnetic resonance imaging following valve-sparing aortic root replacement with tricuspid and bicuspid valve morphology. Eur J Cardiothorac Surg. 2013
14. Kvitting JP, Dyverfeldt P, Sigfridsson A, Franzen S, Wigstrom L, Bolger AF, et al. In vitro assessment of flow patterns and turbulence intensity in prosthetic heart valves using generalized phase-contrast MRI. J Magn Reson Imaging. 2010; 31(5):1075–1080. [PubMed: 20432341]
15. Demers P, Miller DC. Simple modification of "T. David-V" valve-sparing aortic root replacement to create graft pseudosinuses. Ann Thorac Surg. 2004; 78(4):1479–1481. [PubMed: 15464530]
16. Markl M, Harloff A, Bley TA, Zaitsev M, Jung B, Weigang E, et al. Time-resolved 3D MR velocity mapping at 3T: improved navigator-gated assessment of vascular anatomy and blood flow. J Magn Reson Imaging. 2007; 25(4):824–831. [PubMed: 17345635]
17. Sievers HH, Schmidtke C. A classification system for the bicuspid aortic valve from 304 surgical specimens. J Thorac Cardiovasc Surg. 2007; 133(5):1226–1233. [PubMed: 17467434]

18. Stalder AF, Russe MF, Frydrychowicz A, Bock J, Hennig J, Markl M. Quantitative 2D and 3D phase contrast MRI: optimized analysis of blood flow and vessel wall parameters. Magn Reson Med. 2008; 60(5):1218–1231. [PubMed: 18956416]

19. Tai NR, Salacinski HJ, Edwards A, Hamilton G, Seifalian AM. Compliance properties of conduits used in vascular reconstruction. Br J Surg. 2000; 87(11):1516–1524. [PubMed: 11091239]

20. Kim SY, Hinkamp TJ, Jacobs WR, Lichtenberg RC, Posniak H, Pifarre R. Effect of an inelastic aortic synthetic vascular graft on exercise hemodynamics. Ann Thorac Surg. 1995; 59(4):981–989. [PubMed: 7695428]

21. Kilner PJ, Yang GZ, Mohiaddin RH, Firmin DN, Longmore DB. Helical and retrograde secondary flow patterns in the aortic arch studied by three-directional magnetic resonance velocity mapping. Circulation. 1993; 88(5 Pt 1):2235–2247. [PubMed: 8222118]

22. Hope MD, Hope TA, Meadows AK, Ordovas KG, Urbania TH, Alley MT, et al. Bicuspid aortic valve: four-dimensional MR evaluation of ascending aortic systolic flow patterns. Radiology. 2010; 255(1):53–61. [PubMed: 20308444]

23. Barker AJ, Markl M, Burk J, Lorenz R, Bock J, Bauer S, et al. Bicuspid aortic valve is associated with altered wall shear stress in the ascending aorta. Circ Cardiovasc Imaging. 2012; 5(4):457–466. [PubMed: 22730420]

24. Della Corte A, Bancone C, Conti CA, Votta E, Redaelli A, Del Viscovo L, et al. Restricted cusp motion in right-left type of bicuspid aortic valves: a new risk marker for aortopathy. J Thorac Cardiovasc Surg. 2012; 144(2):360–369. 9, e1. [PubMed: 22050982]

25. Kang JW, Song HG, Yang DH, Baek S, Kim DH, Song JM, et al. Association between bicuspid aortic valve phenotype and patterns of valvular dysfunction and bicuspid aortopathy: comprehensive evaluation using MDCT and echocardiography. JACC Cardiovasc Imaging. 2013; 6(2):150–161. [PubMed: 23489528]

26. Barker AJ, van Ooij P, Bandi K, Garcia J, Albaghdadi M, McCarthy P, et al. Viscous energy loss in the presence of abnormal aortic flow. Magn Reson Med. 2013; 2(10):24962.

27. Dyverfeldt P, Hope MD, Tseng EE, Saloner D. Magnetic resonance measurement of turbulent kinetic energy for the estimation of irreversible pressure loss in aortic stenosis. JACC Cardiovasc Imaging. 2013; 6(1):64–71. [PubMed: 23328563]

28. Leontyev S, Borger MA, Davierwala P, Walther T, Lehmann S, Kempfert J, et al. Redo aortic valve surgery: early and late outcomes. Ann Thorac Surg. 2011; 91(4):1120–1126. [PubMed: 21276956]

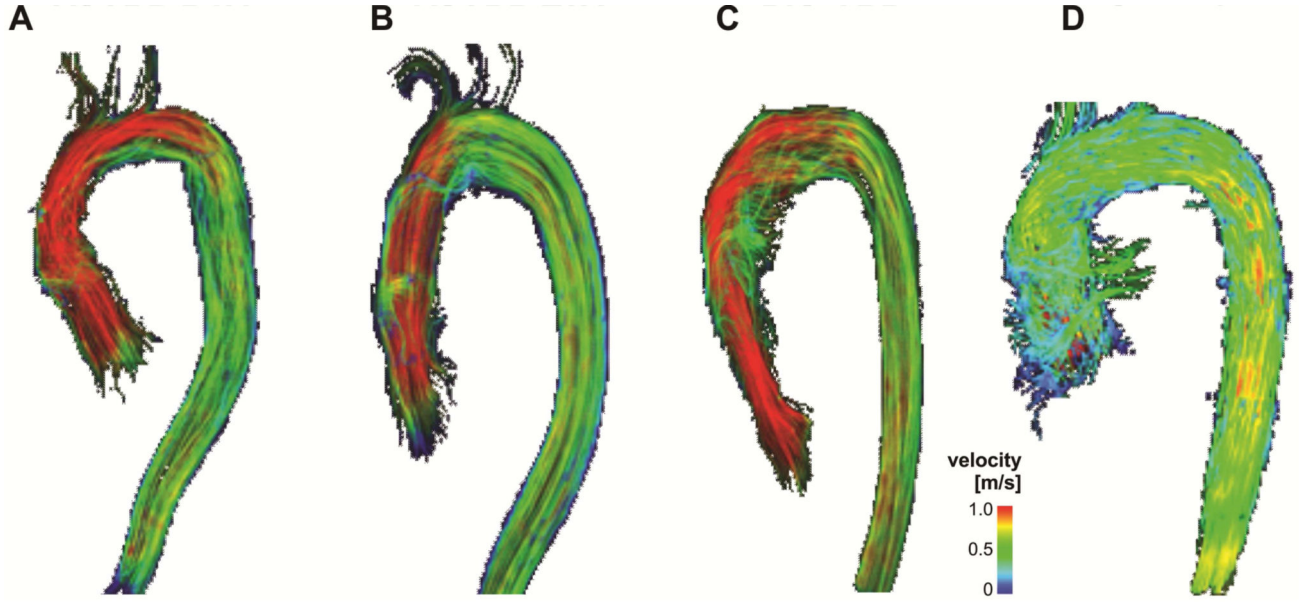

Figure 1.

3D visualization of systolic blood flow characteristics in representative subjects with VSARR BAV (A), VSARR TAV (B), BIO-ARR (C) compared to a and Control (D) subject. VSARR delivers a more physiological blood flow pattern compared to BIO-ARR independent of valve morphology but with a trend more ideal hemodynamics in the VSARR TAV.

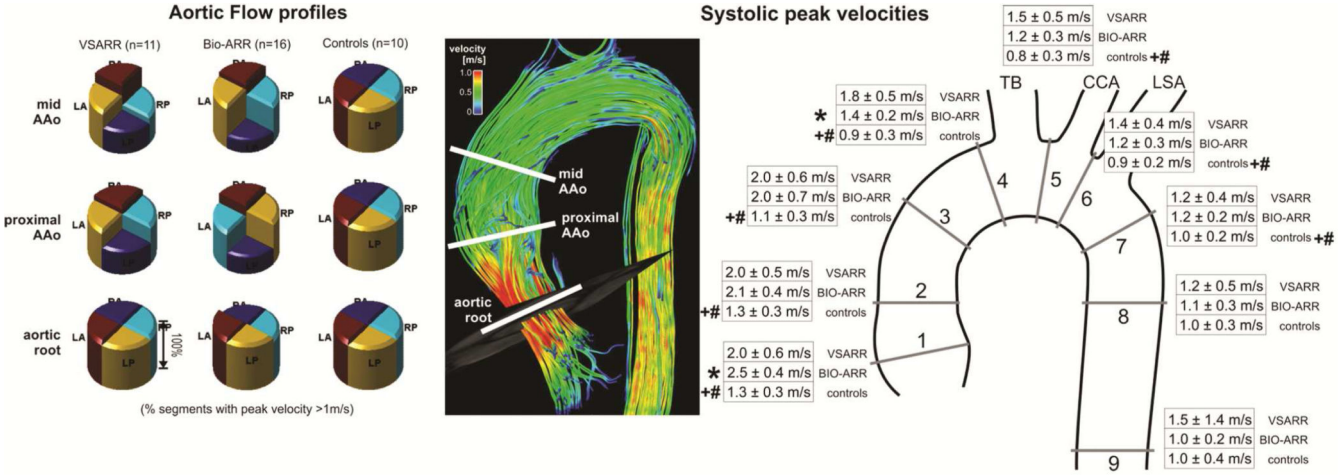

Figure 2.

A. Aortic flow profiles averaged across all three groups (left) and illustration of analysis plane locations in an image showing systolic 3D streamlines in a healthy control subject (right). The individual pie charts represent the percentage of segments in each group containing peak velocities greater than 1m/s. BIO-ARR subjects demonstrated non-uniform flow profiles with eccentrically oriented forward flow jets. VSARR subjects demonstrated elevated velocities with more flow uniformity while controls presented with uniform flow profiles throughout the root and proximal AAo. **B**. Results of quantification of systolic peak velocities in 9 standardized analysis planes distributed across the entire thoracic aorta. Peak systolic velocities are increased across the thoracic aorta for VSARR and BIO-ARR subjects. LA: left anterior, LP: left posterior, RA: right anterior, RP right posterior, TB: Brachiocephalic trunk, CCA: Common carotid artery, LSA: Left subclavian artery.

* significant differences between VSARR and BIO-ARR (two sided t-test, $p<0.05$).

+ significant differences between VSARR and controls (two sided t-test, $p<0.05$).

significant differences between BIO-ARR and controls (two sided t-test, $p<0.05$).

Table 1

Study Cohort Demographic Data

Differences between patient groups were evaluated using the student's t-test.

Cohort	Age (yrs)	Body Mass Index	Systolic Blood Pressure (mmHg)	Diastolic Blood Pressure (mmHg)	HR (bpm)	Maximal Pre-surgical aortic Diameter (cm)	History of Hypertension (%)	History of Dysplipidemia (%)	LVEF (%)
VSARR (n=11)	47±18	25.2±3.4	118±26	65±9	82±10	4.8±1.1	0%	9%	60%
BIO-ARR (n=16)	52±14	29.7±4.4	127±28	75±12	80±11	5.2±0.3	44%	38%	59%
p-value	0.46	0.015	0.75	0.35	0.70	0.005	0.015	0.13	0.39

f = female; yrs = years; SBP = systolic blood pressure, DBP = diastolic blood pressure, HR = heart rate; SOV = sinuses of valsalva diameter, MPA: Maximum presurgical aortic diameter.

Table 2

Surgical characteristics. Differences between BIO-ARR and VSARR surgical characteristics were evaluated using the student's t-test.

Cohort	Perfusion Time (min), median (Q1,Q3)	Cross-Clamp Time (min), median (Q1,Q3)	CABG (%)	Post-Operative Length of Stay (days)	Pre-Discharge Complications (%)	30-Day Mortality (%)
VSARR	204 (202, 224)	185 (176, 194)	0 (%)	5 (5, 6)	1 (11%)	0 (0%)
Bio-ARR	116 (88, 191)	104 (79, 151)	1 (7%)	6 (4, 7)	4 (27%)	0 (0%)
p-value	0.006	0.006	0.43	0.40	0.36	-

Table 3

Results of the semi-quantitative grading of 3D blood flow visualization (helix flow).

	Helix flow AAo	Helix flow arch	Helix flow DAo
Controls	0	0	0
VSARR	0.07±0.27 *	0.07±0.27	0
BIO-ARR	0.9 ±0.6 *β	0.18±0.5	0

* indicates significant difference between VSARR and BIO-ARR groups ($p < 0.05$), β indicates significant difference between Controls and BIO-ARR.